HOKKAIDO UNIVERSITY

Title	The solid-phase partitioning of arsenic in unconsolidated sediments of the Mekong Delta, Vietnam and its modes of release under various conditions
Author(s)	Dang Thuong Huyen; Tabelin, Carlito Baltazar; Huynh Minh Thuan et al.
Citation	Chemosphere, 233, 512-523 https://doi.org/10.1016/j.chemosphere.2019.05.235
Issue Date	2019-10
Doc URL	https://hdl.handle.net/2115/82845
Rights	© 2019. This manuscript version is made available under the CC-BY-NC-ND 4.0 license https://creativecommons.org/licenses/by-nc-nd/4.0/
Rights(URL)	https://creativecommons.org/licenses/by-nc-nd/4.0/
Type	journal article
File Information	Supplementary information-Mekong (Chemosphere-rev1).pdf

Hokkaido University Collection of Scholarly and Academic Papers : HUSCAP

The solid-phase partitioning of arsenic in unconsolidated sediments of the Mekong Delta, Vietnam and its modes of release under various conditions

Dang Thuong Huyen, Carlito Baltazar Tabelin, Huynh Minh Thuan, Dang Hai Dang, Phan Thi Truong, Banthasith Vongphuthone, Masato Kobayashi, and Igarashi Toshifumi

Supplementary information

Summary

This supplement is divided into 5 sections including 6 tables and 11 figures. It provides additional data on the following: (1) descriptions of each sediment sample, (2) elemental compositions of sediments in borehole cores Ph, P-Hu, TT and TL, relative abundances of minerals found in the six borehole cores, solid-phase partitioning of arsenic (As) in Ph, P-Hu, TT and TL, including As leachability with depth under oxic, acidic and reducing conditions, and scanning electron microscopy with energy dispersive X-ray spectroscopy (SEM-EDX) of Fe-oxyhydroxides/oxides and soluble salt-like phases, (3) pH and concentrations of coexisting ions in the leaching experiments using deionized (DI) water (oxic conditions) and the C/S ratio of sediment samples, (4) speciation of As in the leaching experiments using DI water, and (5) principal component analysis (PCA) of results.

1. Brief descriptions of sediment samples

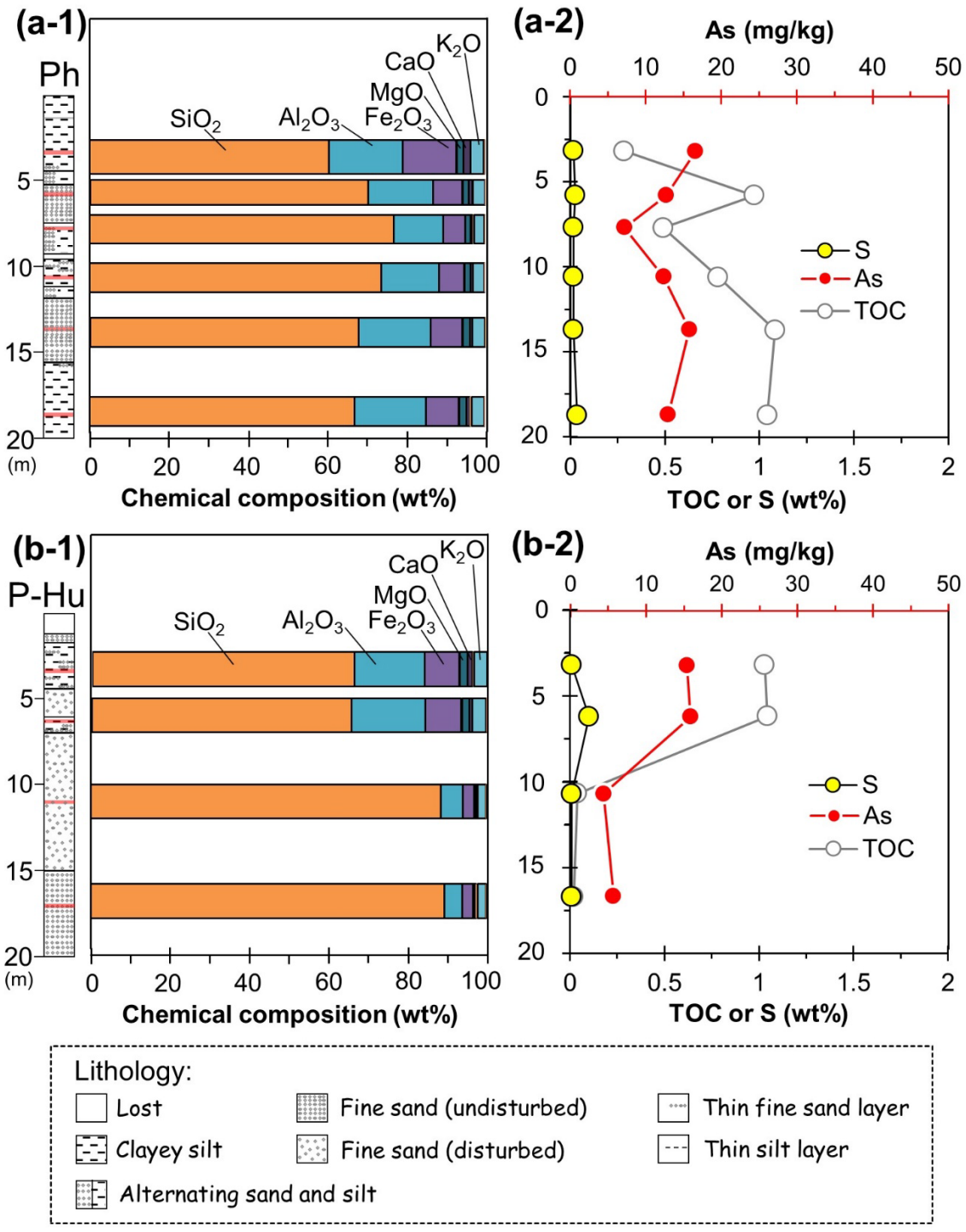
Supplementary Table 1 provides a brief description of the lithology of sediment samples. The particle size distribution of sediments varied with depth and ranged from clayey silt to coarse sand. Two peat layers were also observed in one of the borehole cores (PT) that are approximately 1 m thick.

Supplementary Table 1. Lithology of sediment samples from the six borehole cores.

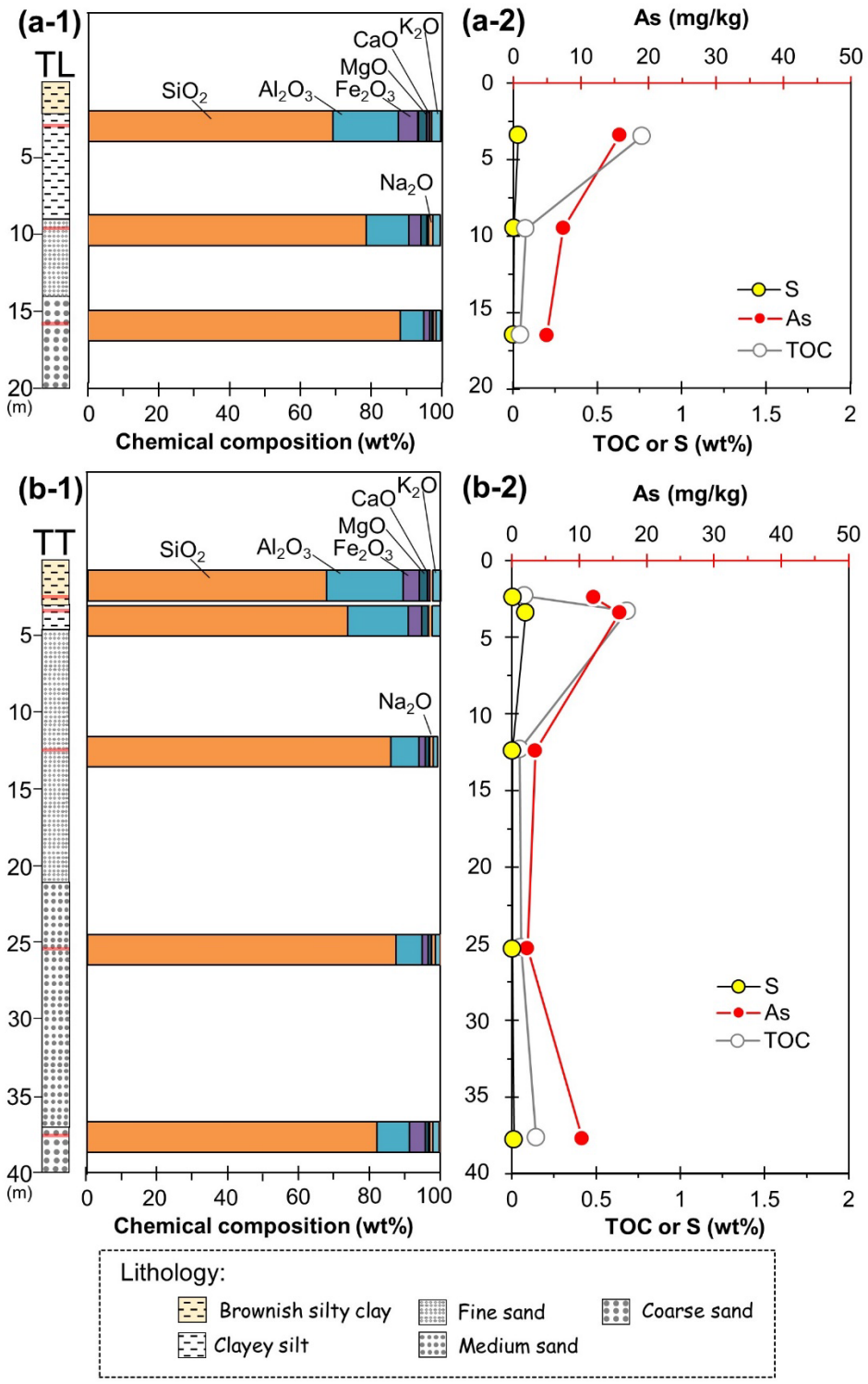
Sample name	Lithology
LS-1	Grey clayey silt
LS-2	Dark grey fine sand with thin brownish grey clayey silt
LS-3	Alternating dark grey fine sand and brownish grey clayey silt (ratio 1:1)
LS-4	Brownish grey clayey silt
LS-5	Grey fine sand (distributed sample)
LS-6	Brownish grey clayey silt
Ph-1	Brownish grey clayey silt
Ph-2	Brownish grey clayey silt, partly including sand
Ph-3	Brownish grey fine sand with thin clayey silt layers
Ph-4	Brownish grey clayey silt
Ph-5	Brownish grey clayey silt, some parts with grey fine sand layers
Ph-6	Brownish grey clayey silt
P-Hu-1	Brownish grey clayey silt and sandy silt
P-Hu-2	Brownish grey clayey silt and sandy silt with a thin grey fine sand layer
P-Hu-3	Grey fine sand (distributed sample)
P-Hu-4	Grey fine sand
PT-1	Grey brownish to reddish clayey silt
PT-2	Dark grey clay with some reddish clayey silt layers
PT-3	Dark grey clay with thin sand layers with some organic matter
PT-4	Dark grey clay with thin sand layers
PT-5	Dark grey clay with fine sand layers
PT-6	Black clayey peat
PT-7	Dark grey fine sand
PT-8	Black clayey peat
PT-9	Reddish-grey clayey containing laterite
PT-10	Dark grey coarse sand
TL-1	Grey clayey silt
TL-2	Dark grey fine sand
TL-3	Dark grey coarse sand
TT-1	Grey-yellowish clayey silt with dark-grey clayey silt layers
TT-2	Dark-gray clayey silt
TT-3	Grey fine sand
TT-4	Grey medium sand
TT-5	Grey coarse sand

2. Chemical compositions, relative mineral abundances and solid-phase partitioning of arsenic

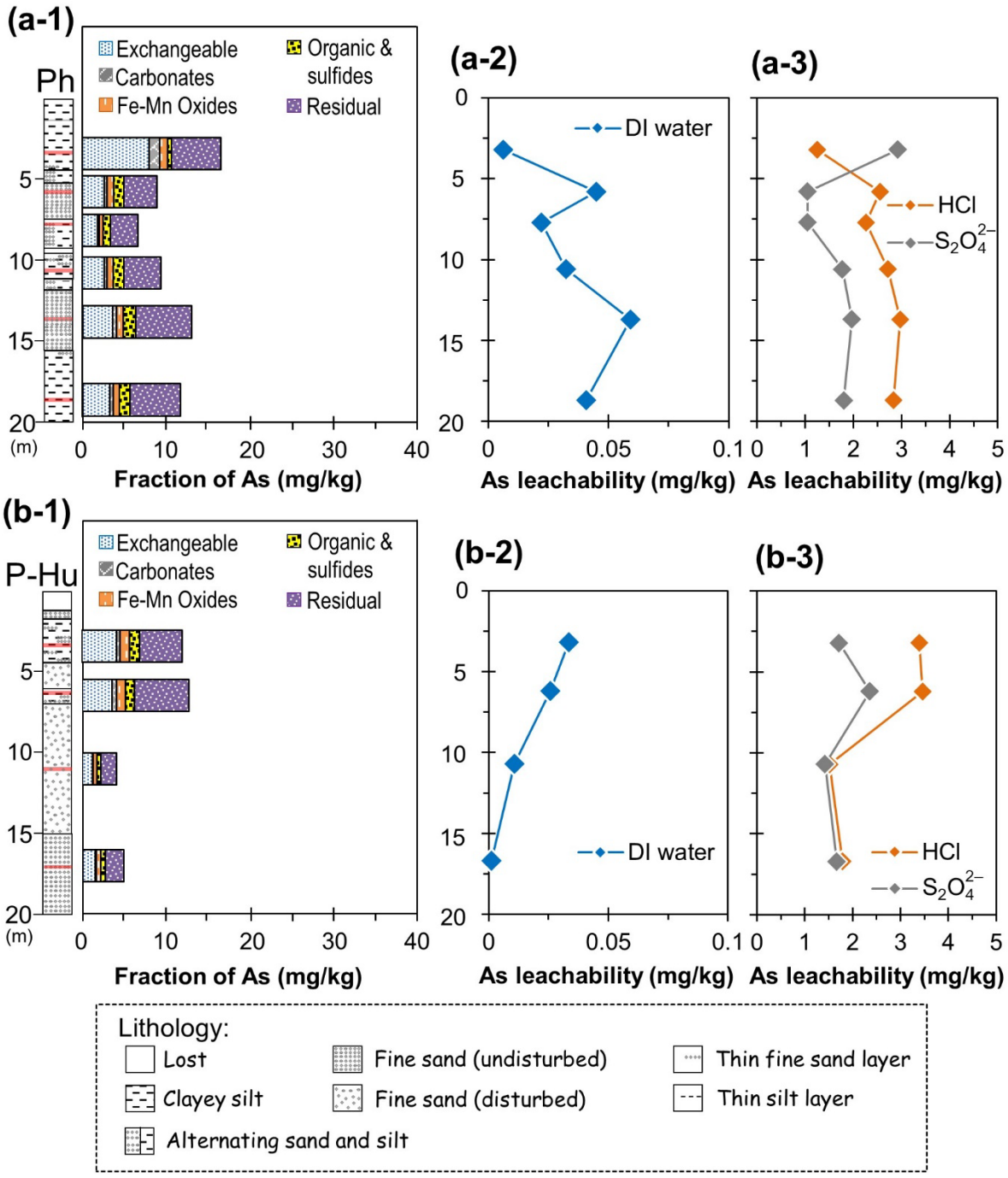
Supplementary Figs. 1 and 2 illustrate the chemical composition of distinct geological features in borehole cores Ph, P-Hu, TT, and TL, including the distribution of As, sulfur (S) and total organic carbon (TOC) with depth, while Supplementary Figs. 3 and 4 show the solid-phase partitioning of As with depth and its leachability under oxic, reducing and acidic conditions. Based on the XRD patterns, the abundance of minerals in the samples were obtained semi-quantitatively using Match!® (Crystal Impact, Germany) and the results are summarized in Supplementary Tables 2–4. The results showed that most of the samples are composed mainly of quartz, anorthite, muscovite, clinochlore and kaolinite with minor to trace amounts of carbonates, soluble salts (e.g., gypsum and KCl) (Supplementary Fig. 5), Fe-oxyhydroxides/oxides (Supplementary Figs. 6 and 7) and pyrite (Supplementary Fig. 5).



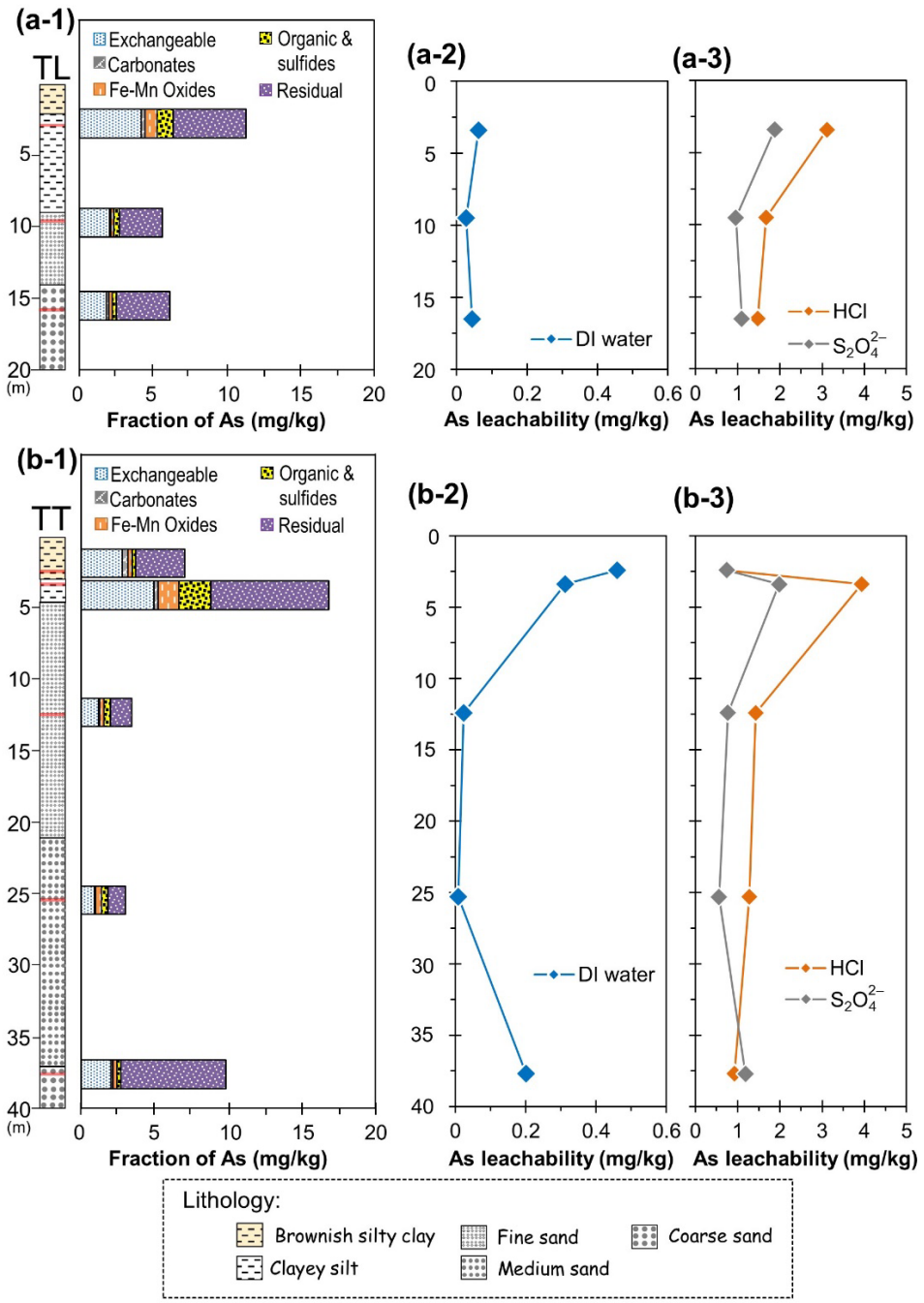
Supplementary Fig. 1. Chemical compositions of distinct lithological features in borehole cores from Hau River (Ph and P-Hu): (a-1) variation of major chemical components in Ph with depth, (a-2) distribution of trace components (As, S and TOC) in Ph with depth, (b-1) variation of major chemical components in P-Hu with depth, and (b-2) distribution of trace components (As, S and TOC) in P-Hu with depth.



Supplementary Fig. 2. Chemical compositions of distinct lithological features in borehole cores from the Tien River (TL and TT): (a-1) variation of major chemical components in TL with depth, (a-2) distribution of trace components (As, S and TOC) in TL with depth, (b-1) variation of major chemical components in TT with depth, and (b-2) distribution of trace components (As, S and TOC) in TT with depth.



Supplementary Fig. 3. Solid-phase partitioning and leaching behaviors of As in distinct lithological features of borehole cores from the Hau River under various conditions: (a-1) distribution of As in exchangeable, carbonate, Fe-Mn oxides (reducible), organic and sulfides, and residual phases in sediment samples from Ph, (a-2) leaching of As with depth under oxidizing (DI water) conditions in Ph, (a-3) leaching of As with depth under acidic (HCl) and reducing ($S_2O_4^{2-}$) conditions in Ph, (b-1) distribution of As in exchangeable, carbonate, Fe-Mn oxides (reducible), organic and sulfides, and residual phases in sediment samples from P-Hu, (b-2) leaching of As with depth under oxidizing (DI water) conditions in P-Hu, (b-3) leaching of As with depth under acidic (HCl) and reducing ($S_2O_4^{2-}$) conditions in P-Hu.



Supplementary Fig. 4. Solid-phase partitioning and leaching behaviors of As in distinct lithological features of borehole cores from the Tien River under various conditions: (a-1) distribution of As in exchangeable, carbonate, Fe-Mn oxides (reducible), organic and sulfides, and residual phases in sediment samples from TL, (a-2) leaching of As with depth under oxidizing (DI water) conditions in TL, (a-3) leaching of As with depth under acidic (HCl) and reducing ($S_2O_4^{2-}$) conditions in TL, (b-1) distribution of As in exchangeable, carbonate, Fe-Mn oxides (reducible), organic and sulfides, and residual phases in sediment samples from TT, (b-2) leaching of As with depth under oxidizing (DI water) conditions in TT, (b-3) leaching of As with depth under acidic (HCl) and reducing ($S_2O_4^{2-}$) conditions in TT.

Supplementary Table 2. Relative abundance of minerals in samples from borehole cores Ph and P-Hu.

Sample	Depth (m)	Relative abundance (wt.%)											
		Qz	An	Ab	Kln	Ms	Clc	Cal	Dol	Py	Gt	Hem	Gp
Ph-1	2.8–3.0	60.9	13.1	0.6	6.8	4.8	10.2	2.8	–	0.3	0.5	–	–
Ph-2	7.2–7.4	64.7	14.4	–	2.4	9.7	6.9	–	1.5	–	0.1	0.3	–
Ph-3	11.6–11.8	79	13.1	–	2.4	1.7	1.7	0.4	0.5	–	1.6	–	–
Ph-4	14.7–14.9	71.9	17.9	–	0.4	6	2.7	–	0.3	–	0.2	0.7	–
Ph-5	16.2–16.4	68.1	8.3	1.6	4.8	12.2	4.3	–	0.2	0.1	–	0.3	–
Ph-6	19.1–19.3	68.4	10.3	1.1	5	11.3	3	–	–	–	0.7	0.3	–
P-Hu-1	3.2–3.4	58.4	11.7	0.2	5.2	13.6	7	–	1.9	0.2	0.7	1	–
P-Hu-2	6.2–6.4	59	10.7	1.5	6.4	16	4.2	–	1.4	–	–	0.8	–
P-Hu-3	10.7–10.9	73.5	10.3	2.4	0.4	3	9.2	–	1.1	–	–	0.1	–
P-Hu-4	16.7–16.9	86.4	10.4	–	1	2.2	–	–	–	–	–	–	–

*Quartz: Qz; Anorthite: An; Albite: Ab; Muscovite: Ms; Kaolinite: Kln; Clinochlore: Clc; Calcite: Cal; Dolomite: Dol; Pyrite: Py; Goethite: Gt; Hematite: Hem; Gypsum: Gp; "–": Not detected

Supplementary Table 3. Relative abundance of minerals in samples from borehole cores LS and PT.

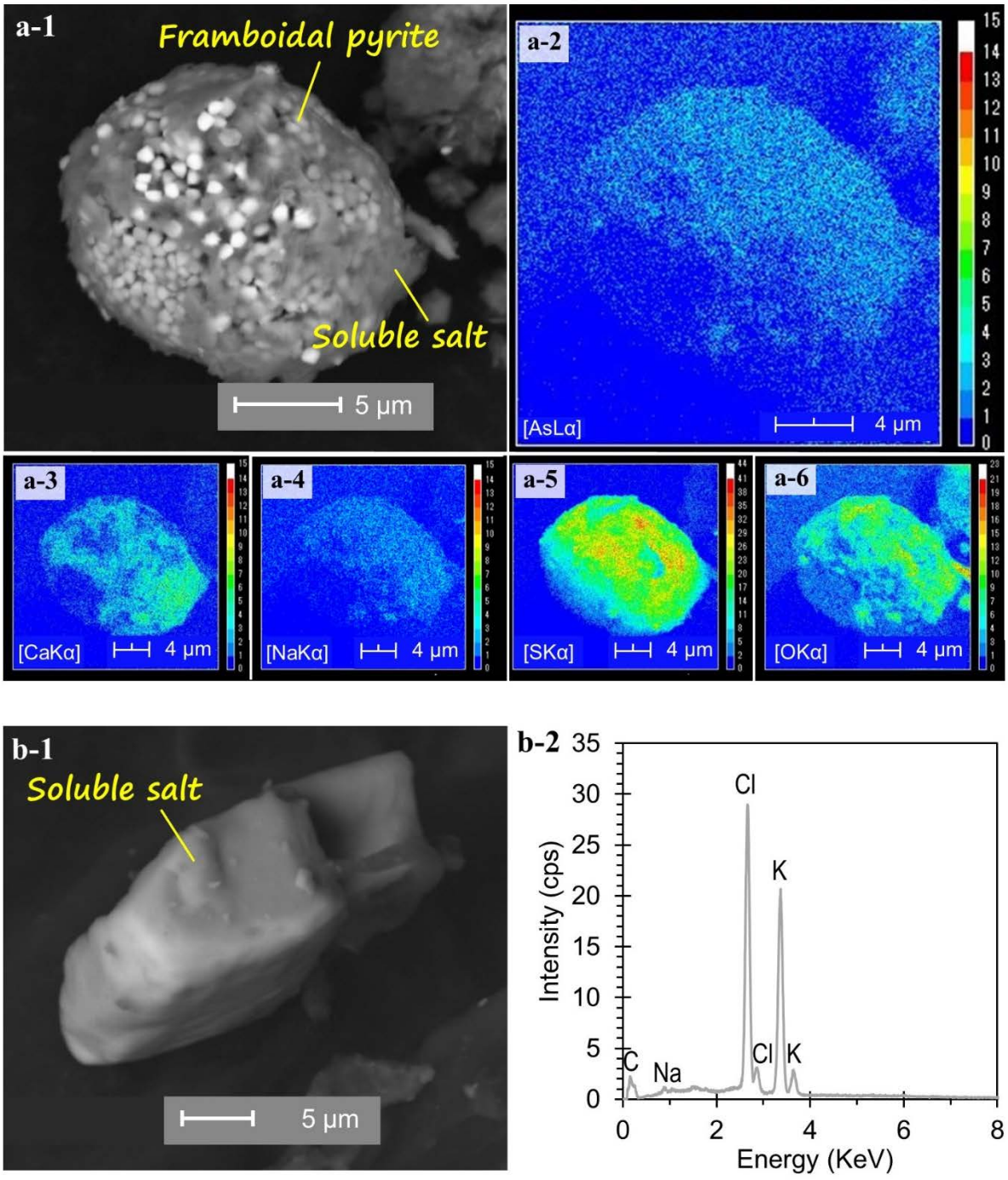
Sample	Depth (m)	Relative abundance (wt.%)											
		Qz	An	Ab	Kln	Ms	Clc	Cal	Dol	Py	Gt	Hem	Gp
LS-1	3.2–3.4	64.1	8.3	–	5.4	14.1	3.7	–	–	2.2	1.9	–	0.3
LS-2	5.8–6.0	73.9	8.2	7.6	–	6.6	2.6	–	–	–	0.3	0.4	0.4
LS-3	7.7–7.9	72.2	18.9	–	3.1	1.1	3.8	0.3	–	0.6	–	–	–
LS-4	10.2–10.7	59.8	8	–	8.5	14.5	5.7	–	1.4	–	–	1.7	0.4
LS-5	13.7–13.9	72.9	18.6	1.2	3.3	3.8	–	–	–	0.2	–	–	
LS-6	18.7–18.9	56.9	5.7	1.9	7.2	18	5.7	–	2.4	–	1.7	–	0.5
PT-1	1.2–1.3	61.6	7.5	2.8	6.1	13.8	5.5	–	–	–	2.7	–	–
PT-2	4.2–4.3	57.2	5.7	2.9	10.3	7.4	12.4	1.1	–	–	1.7	–	1.1
PT-3	6.4–6.5	71.6	15.3	–	4.8	0.7	4.8	0.7	–	1	1.1	–	–
PT-4	11.2–11.3	57.2	13.8	–	10.1	0.8	9	1.6	3.4	1.4	2	0.7	–
PT-5	17.6–17.7	81.2	17.4	–	0.3	1.1	–	–	–	–	–	–	–
PT-6	19.2–19.3	39.8	10.1	6.6	11.7	6	15.2	0.8	–	6	–	1.2	4.3
PT-7	21.6–21.7	80.1	16.1	1.2	1.2	–	0.1	–	–	–	–	1.4	–
PT-8	24.5–24.6	41.2	2.7	2.7	14.2	22.1	11	0.5	2.4	2.3	–	–	0.9
PT-9	28.3–28.4	59.5	14.8	–	12.3	3.8	5.6	–	2.7	1.3	–	–	–
PT-10	38.1–38.2	82.4	15.4	–	1	1.2	–	–	–	–	–	–	

*Quartz: Qz; Anorthite: An; Albite: Ab; Muscovite: Ms; Kaolinite: Kln; Clinochlore: Clc; Calcite: Cal; Dolomite: Dol; Pyrite: Py; Goethite: Gt; Hematite: Hem; Gypsum: Gp; "–": Not detected

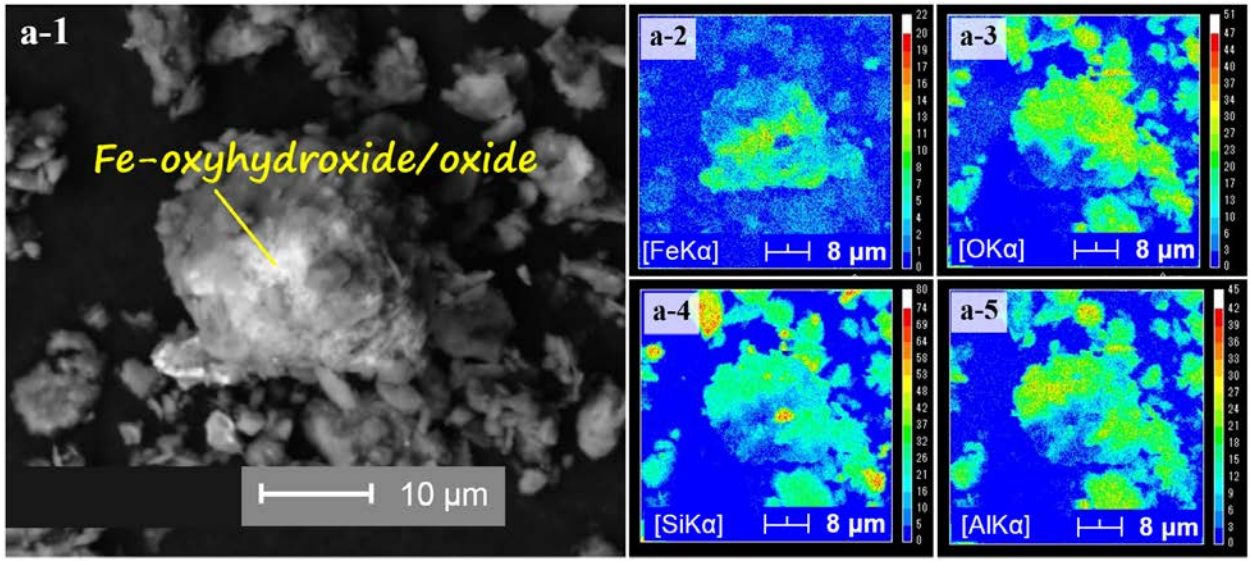
Supplementary Table 4. Relative abundance of minerals in samples from borehole cores TL and TT.

Sample	Depth (m)	Relative abundance (wt.%)											
		Qz	An	Ab	Kln	Ms	Clc	Cal	Dol	Py	Gt	Hem	Gp
TL-1	3.4–3.5	60.3	16.3	0.1	6.6	2.9	12.6	0.6	–	0.6	–	–	–
TL-2	9.5–9.6	64.8	17.8	–	5	3.1	4.8	0.7	3.3	0.6	–	–	–
TL-3	16.5–16.6	88.9	4	6.2	–	–	–	–	–	–	–	0.8	–
TT-1	2.4–2.5	61.1	6.2	–	7.7	19.5	2.9	0.8	–	–	0.1	1.6	–
TT-2	3.4–3.5	76.5	13.7	–	4.5	0.8	4.1	0.1	–	0.1	–	0.2	–
TT-3	12.4–12.5	87.4	9.4	1.9	0.5	0.8	–	–	–	–	–	–	–
TT-4	25.3–25.4	85.2	12.3	1	–	1.1	–	0.4	–	–	–	–	–
TT-5	37.7–37.8	85.2	12.2	–	–	2.6	–	–	–	–	–	–	–

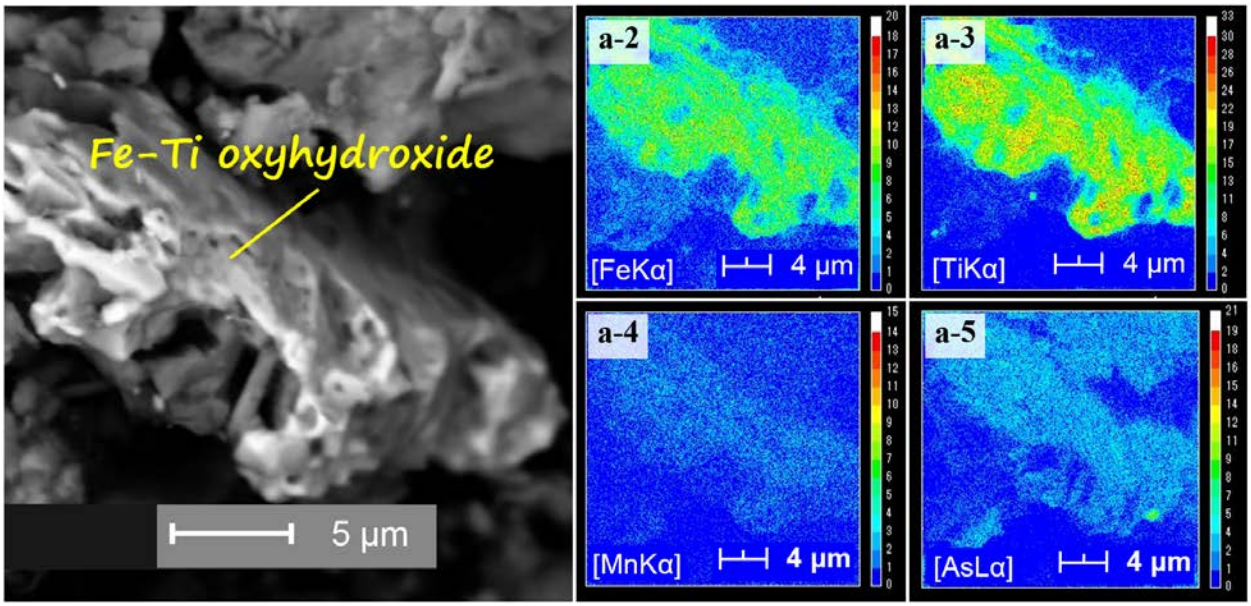
*Quartz: Qz; Anorthite: An; Albite: Ab; Muscovite: Ms; Kaolinite: Kln; Clinochlore: Clc; Calcite: Cal; Dolomite: Dol; Pyrite: Py; Goethite: Gt; Hematite: Hem; Gypsum: Gp; "–": Not detected



Supplementary Fig. 5. SEM photomicrographs of As-bearing soluble salt and framboidal pyrite (a-1) and the corresponding elemental maps of As (a-2), Ca (a-3), Na (a-4), S (a-5), and O (a-6), and SEM photomicrographs of a salt-like particle composed mainly of KCl (b-1) and the EDS spectrum of the particle (b-2).



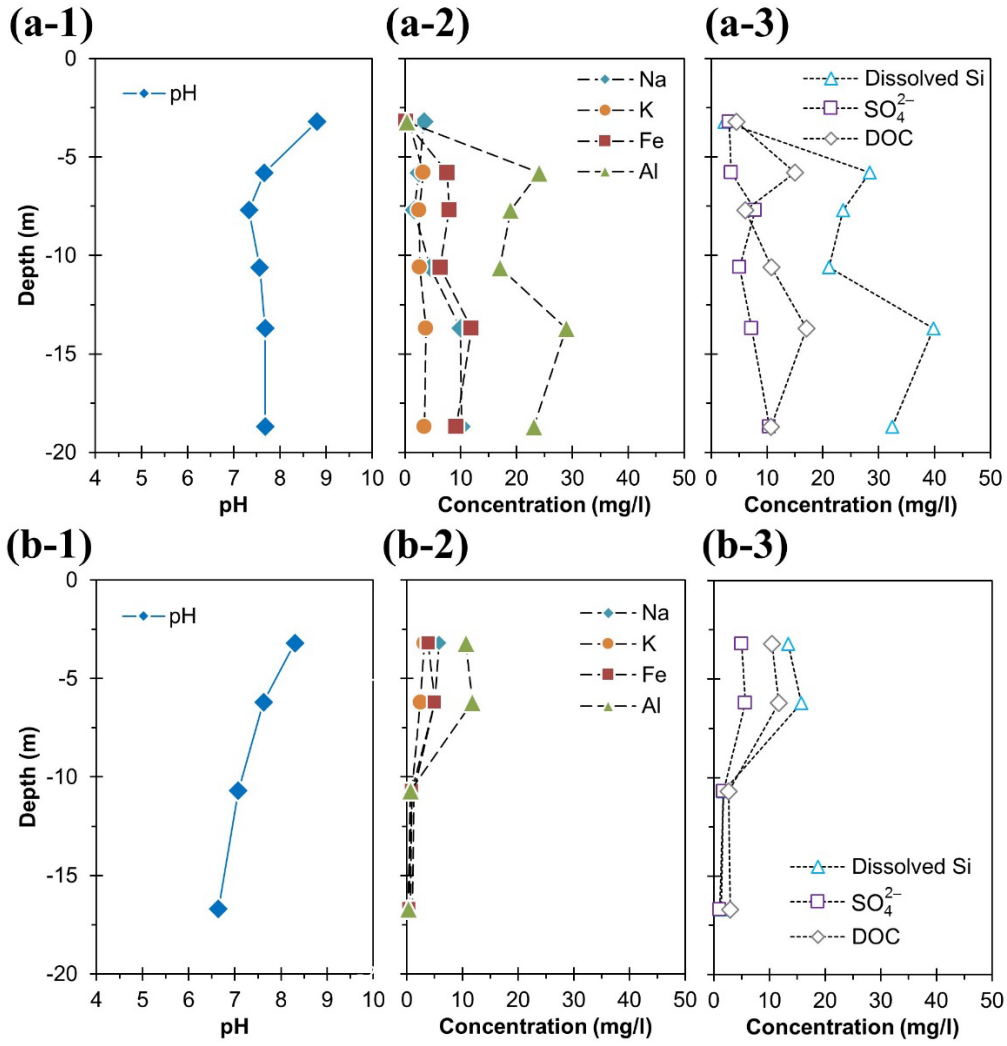
Supplementary Fig. 6. SEM photomicrographs of Fe-oxyhydroxide/oxide (a-1) and the corresponding elemental maps of Fe (a-2), O (a-3), Si (a-4), and Al (a-5).



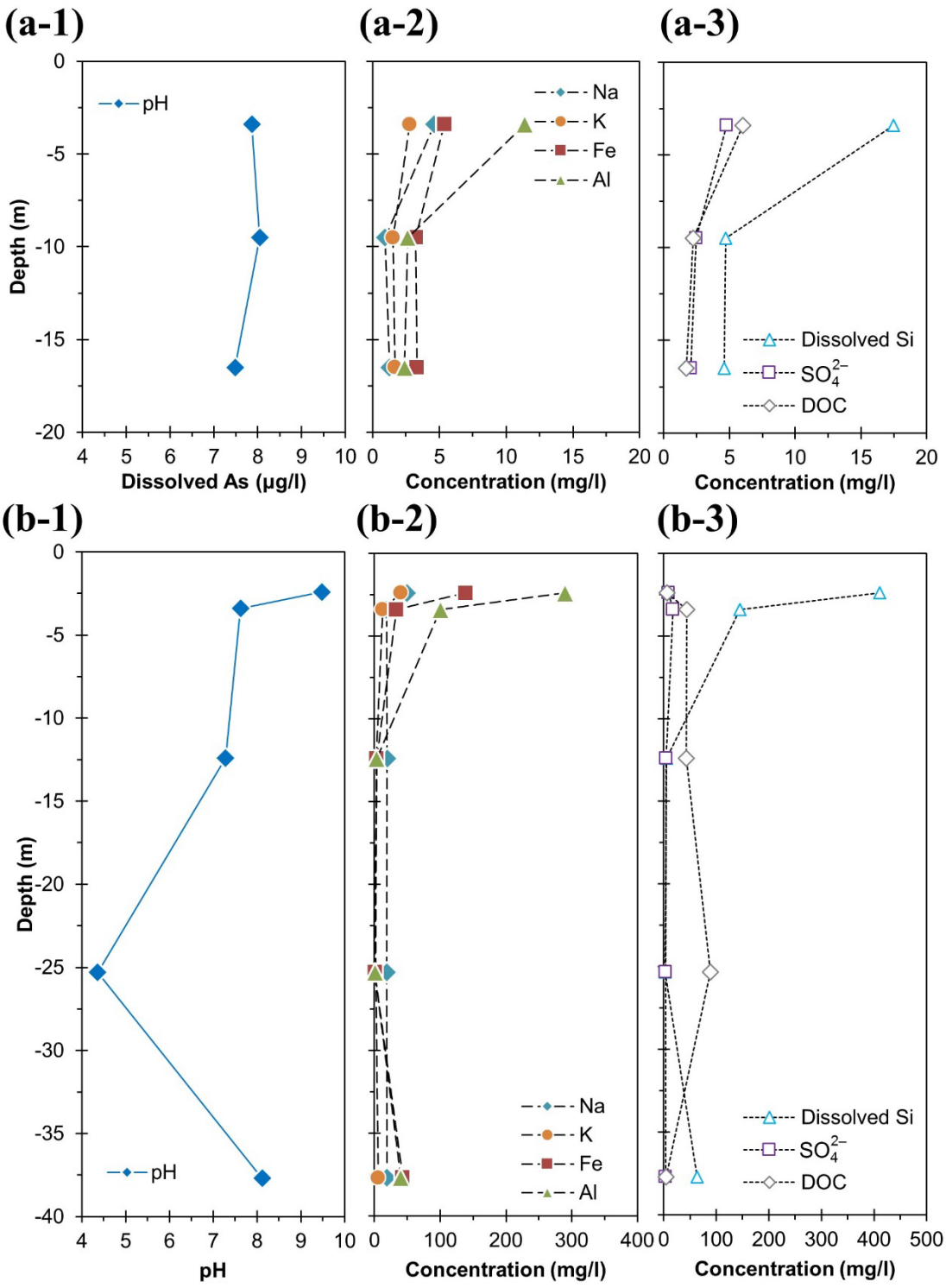
Supplementary Fig. 7. SEM photomicrographs of a Fe-oxyhydroxide/oxide particle-containing Ti, Mn and As (a-1) and the corresponding elemental maps of Fe (a-2), Ti (a-3), Mn (a-4), and As (a-5).

3. pH and concentrations of coexisting ions in the leaching experiments using DI water

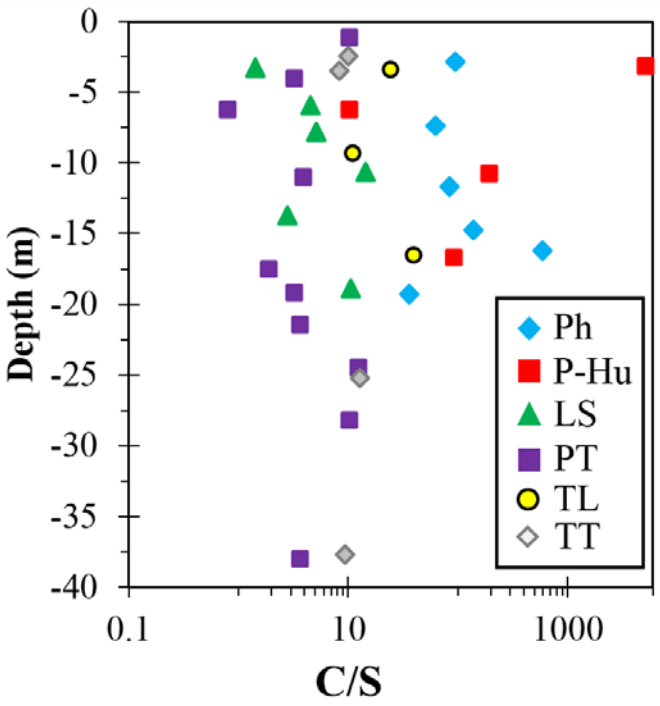
The pH and concentrations of coexisting ions of leachates of samples from Ph, P-Hu, TL and TT leached in DI water are shown in Supplementary Figs. 8 and 9. The pH values ranged from 4 to 10 and the concentrations of coexisting ions varied with depth and sampling location. Supplementary Fig. 10 illustrates the C/S ratio of sediments, a parameter widely used to infer whether sediments are formed under marine/brackish or freshwater environments.



Supplementary Fig. 8. Vertical distribution of pH and coexisting ions from the leaching experiments using DI water: (a-1) pH with depth in Ph, (a-2) Na^+, K^+, Fe and Al concentration with depth in Ph, (a-3) dissolved Si, SO_4^{2-}, DOC concentrations with depth in Ph, (b-1) pH with depth in P-Hu, (b-2) Na^+, K^+, Fe and Al concentrations with depth in P-Hu, (b-3) dissolved Si, SO_4^{2-} and DOC concentrations with depth in P-Hu.



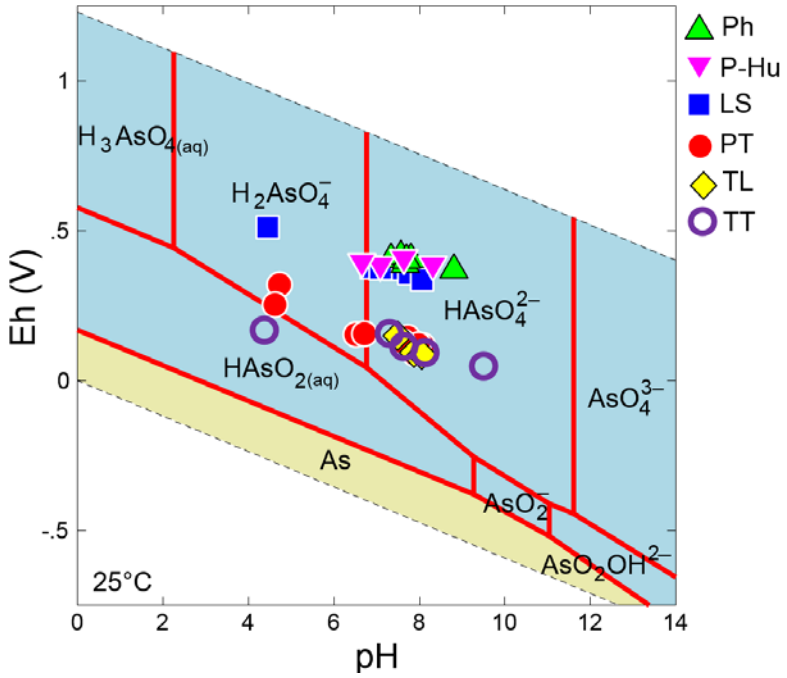
Supplementary Fig. 9. Vertical distribution of pH and coexisting ions from the leaching experiments using DI water: (a-1) pH with depth in TL, (a-2) Na^+, K^+, Fe and Al concentrations with depth in TL, (a-3) dissolved Si, SO_4^{2-}, DOC concentrations with depth in TL, (b-1) pH with depth in TT, (b-2) Na^+, K^+, Fe and Al concentrations with depth in TT, (b-3) dissolved Si, SO_4^{2-} and DOC concentrations with depth in TT.



Supplementary Fig. 10. C/S ratio with the depth of sediments in the six borehole cores.

4. Speciation of arsenic in the leaching experiments using DI water

Supplementary Fig. 11 illustrates the speciation of As in leachates from the leaching experiments using DI water. Except for one sample from TT, As in the leachates most likely exist as various oxyanions of arsenate (As^{V}).



Supplementary Fig. 11. Eh-pH predominance diagram of As at 25°C, 1.013 bars, and activity of As = 10^{-4}. Data points represent the actual leachate pH and Eh values measured during the leaching experiments in DI water.

5. Principal component analysis of results

For the PCA of the chemical properties of sediments, 11 variables (SiO_2, Al_2O_3, Fe_2O_3, MgO, CaO, Na_2O, K_2O, S, As, TOC and LOI) of the 34 samples were used, and the calculated loadings and contributions are presented in Supplementary Table 5. The significance of the first principal component (PC 1) is discussed in detail in the main text while in this section the second and third principal components (PC 2 and 3) will be discussed in more detail. The second principal component (PC 2) explained 24.37% of the total inertia and had high loadings of SiO_2, Na_2O, and S. This principal component could be related to the incorporation of Na in the sediments; that is, Na is found with both SiO_2 as albite (Supplementary Tables 2–4) and S as soluble salt-like phases (e.g., mirabilite) (Supplementary Fig. 5). Soluble salts were found in the sediments most likely because the aquifer was formed in brackish and/or marine environments.

This deduction is supported by the ratio in wt.% of organic carbon content to sulfur content (C/S) of the sediments, a parameter used by many researchers to determine how modern and ancient sediments were formed (Berner and Raiswell, 1984; Sampei et al., 1997). Sediments formed under freshwater conditions are typically characterized by C/S values >10 whereas those formed under saline conditions have C/S < 10. As illustrated in Supplementary Fig. 11, about one-third of the sediment samples (mostly those in peat and clayey silt) had C/S < 10, indicating that they were likely deposited in brackish and/or marine environments. These observations were also consistent with the study of Nguyen et al. (2000) who reported that the Vietnamese-side of the Mekong Delta was submerged in seawater around 5000–6000 yrs. BP, which caused the widespread deposition of marine sediments in the delta. The third principal factor (PC 3) captured 9.47% of the total inertia and had high positive loadings of Al_2O_3 and MgO together with the negative loadings of S and TOC. This principal component clearly contrasted Al_2O_3 and MgO from TOC and S and could be related to processes that occurred during the formation of the Mekong Delta. Enhanced formation of dolomite in sedimentary rocks has been reported by several authors due to microbial sulfate reduction that consumes organic carbon (Radke and Mathis, 1980). Similarly, organic-rich and anoxic environments have been reported to promote the dissolution of alumino-silicates via the formation of silica/alumina organic complexes (Bennett et al., 1991), so higher TOC and S would be correlated to lower Al_2O_3 and MgO contents of sediments.

Supplementary Table 5. Rotated factor loadings and contributions of principal components (PC).

Parameters	**PC 1**	**ctr$_1$**	**PC 2**	**ctr$_2$**	**PC 3**	**ctr$_3$**
SiO_2	-0.237	1.4	**0.451**	7.6	0.266	6.8
Al_2O_3	**0.334**	2.1	0.079	0.2	**0.489**	23
Fe_2O_3	**0.349**	2.3	-0.287	3.1	0.098	0.9
MgO	**0.351**	2.3	0.240	2.1	**0.343**	11
CaO	0.261	1.3	-0.212	1.7	0.084	0.7
Na_2O	-0.008	0.0	**0.550**	11	0.253	6.2
K_2O	**0.361**	2.4	-0.142	0.8	0.226	4.9
S	0.272	1.4	**0.313**	3.7	*-0.458*	20
As	**0.358**	2.4	-0.145	0.8	-0.110	1.2
TOC	**0.318**	1.9	0.272	2.8	*-0.423*	17
LOI	0.293	1.6	0.300	3.4	-0.199	3.8
Eigenvalue	5.4		2.68		1.04	
Inertia explained	49.07		24.37		9.47	
Cumulative	49.07		73.43		82.9	

The **positive** important contributions are in bold, and the *negative* important contributions are italicized. For convenience, contributions (ctr) have been multiplied by 100.

Supplementary Table 6 summarizes the PCA results using 16 parameters (pH, EC, Eh, Na^+, K^+, Mg^{2+}, Ca^{2+}, Fe, Al, dissolved Si, As, Cl^-, NO_3^-, SO_4^{2-}, HCO_3^- and DOC) of 34 leachate samples from the experiments with DI water.

Supplementary Table 6. Rotated factor loadings and contributions of principal components (PC).

Parameters	**PC 1**	**ctr$_1$**	**PC 2**	**ctr$_2$**	**PC 3**	**ctr$_3$**
pH	0.098	0.1	*-0.332*	3.6	**0.398**	6.6
EC	-0.087	0.1	**0.441**	6.3	0.200	1.7
Eh	-0.197	0.5	**0.280**	2.5	0.123	0.6
Na^+	**0.326**	1.4	0.083	0.2	-0.172	1.2
K^+	**0.359**	1.7	0.059	0.1	0.059	0.1
Mg^{2+}	**0.286**	1.1	**0.278**	2.5	0.157	1.0
Ca^{2+}	-0.044	0.0	**0.469**	7.1	0.186	1.4
Fe	**0.338**	1.5	-0.046	0.1	0.158	1.0
Al	**0.351**	1.7	0.001	0.0	0.055	0.1
Dissolved Si	**0.359**	1.7	0.018	0.0	0.057	0.1
As	**0.314**	1.3	-0.021	0.0	-0.016	0.0
Cl^-	0.196	0.5	0.044	0.1	*-0.479*	9.6
NO_3^-	**0.272**	1.0	0.095	0.3	-0.043	0.1
SO_4^{2-}	0.042	0.0	**0.529**	9.0	-0.061	0.2
HCO_3^-	0.181	0.4	-0.123	0.5	**0.424**	7.5
DOC	0.114	0.2	-0.009	0.0	*-0.498*	10
Eigenvalue	7.42		3.1		2.4	
Inertia explained	46.36		19.4		14.98	
Cumulative	46.36		65.76		80.75	

The **positive** important contributions are in bold, and the *negative* important contributions are italicized. For convenience, contributions (ctr) have been multiplied by 100.

References

Bennett, P.C., Siegel, D.I., Hill, B.M., Glaser, P.H., 1991. Fate of silicate minerals in a peat bog. Geology 19, 328–331.

Berner, R.A., Raiswell, R., 1984. TOC/TS method for distinguishing freshwater from marine sedimentary rocks. Geology 12, 365–368.

Nguyen, V.L., Ta, T.K.O., Tateishi, M., 2000. Late Holocene depositional environments and coastal evolution of the Mekong River Delta, Southern Vietnam. J. Asian Earth Sci. 18, 427–439.

Radke, B.M., Mathis, R.L., 1980. On the formation and occurrence of saddle dolomite. J. Sediment. Res. 50, 1149–1168.

Sampei, Y., Matsumoto, E., Kamei, T., Tokuoka, T., 1997. Sulfur and organic carbon relationship in sediments from coastal brackish lakes in the Shimane peninsula district, southwest Japan. Geochem. J. 31, 245–262.